Chinese Chemical Letters 33 (2022) 783–787

Contents lists available at ScienceDirect

Chinese Chemical Letters

journal homepage: www.elsevier.com/locate/cclet

Carbon dots confined in 3D polymer network: Producing robust room temperature phosphorescence with tunable lifetimes

Yingxiang Zhai, Ping Wang, Xinyue Zhang, Shouxin Liu, Jian Li, Zhijun Chen*, Shujun Li*

Key Laboratory of Bio-based Material Science & Technology, Ministry of Education, Northeast Forestry University, Harbin 150040, China

ARTICLE INFO

Article history:
Received 31 May 2021
Revised 9 August 2021
Accepted 15 August 2021
Available online 20 August 2021

Keywords:
Carbon dots
3D polymer network
Room temperature phosphorescence
Tunable lifetime
Generality

ABSTRACT

Room temperature phosphorescence (RTP) is important in both organic electronics and encryption. Despite rapid advances, a universal approach to robust and tunable RTP materials based on amorphous polymers remains a formidable challenge. Here, we present a strategy that uses three-dimensional (3D) confinement of carbon dots in a polymer network to achieve ultra-long lifetime phosphorescence. The RTP of the as-obtained materials was not quenched in different polar organic solvents and the lifetime of the RTP was easily tuned by adjusting the amount of crosslinking or varying the drying temperature of the 3D molecular network. As a demonstration of potential application, as-obtained RTP materials were successfully used to prepare RTP fibres for flexible textiles. As well as bringing to light a fundamental principle for the construction of polymer materials with RTP, we have endowed traditional carbon dots and polymers with fresh features that will expand potential applications.

Room-temperature phosphorescence (RTP) by organic compounds, which is characterized by long-lived triplet excitons and a very large Stokes shift, is attracting increased attention [1-4]. Typically, efficient RTP emission by organic compounds requires two basic attributes: facilitation of intersystem crossing from the excited singlet state to the lowest excited triplet state and inhibition of non-radiative transition from the first excited triplet state to the ground state [5-9]. Emission from an excited triplet state can, however, easily be quenched at room temperature under ambient conditions [10-16]. Fortunately, quenching can be prevented by embedding the phosphor in a rigid polymer matrix [17-20]. As well as restraining molecular vibrations and rotations of the phosphor, the polymer matrix also reduces the quenching effects of atmospheric oxygen and moisture, allowing the triplet excitons of the organic compound to survive long enough for emission at room temperature [21,22]. Research into polymer-based RTP materials increased significantly following a report of dual-emissive polymer materials by Fraser and co-workers in 2009 [23].

Amongst these polymer-based RTP materials, carbon dots (CDs)-doped polymers have received particular attention because they are easy to prepare and have readily tunable emission [24-31]. Such materials have mainly been prepared by physical blending of CDs with a polymer matrix, such as cellulose [32], polyvinyl alcohol [33-39], silica gel [40], polyurethane [41], polyacrylic acid or polyacrylamide [42], using solvent engineering. In this process, the CDs and polymer are dispersed in solvent and mixed evenly, followed by evaporation of the solvent to give the CDs-doped polymer-based RTP materials [43]. RTP materials prepared in this way, however, have only weak interactions between the CDs and the polymer matrix, which means that the CDs are easily separated from the matrix, leading to weakened RTP emission. Additionally, there are very few reports of CDs-doped polymer-based RTP materials with tunable lifetimes, although these are crucial for high-resolution anti-counterfeiting methods and data encryption. To address this need, we have developed a general 3D confinement strategy for preparing robust polymer-based CDs-doped RTP materials by *in situ* crosslinking of CDs into a 3D polymer network. Firstly, the sustainable CDs were obtained *via* hydrothermal treatment of carboxymethylcellulose (CMC) and ethylenediamine. Next, the hydrogel precursor is gelated, trapping the CDs *in situ* in the 3D polymer network of the hydrogel. A robust polymer-based RTP material is then obtained by simply drying/freezing-dry the hydrogel. Specifically, carboxymethylcellulose (CMC) CDs were polymerized *in situ* with *N,N'*-methylenebisacrylamide (MBA, crosslinker) and acrylamide (AM, monomer) using radical chemistry to produce CMC CDs embedded in a three-dimensional polyacrylamide (PAM) hydrogel network (Scheme 1) [44-46]. RTP materials (CMC CDs@PAM) were easily obtained after drying the hydrogel. Interestingly, the lifetime of the CMC CDs@PAM composites can be flexibly tuned by altering the crosslinking density or by varying the drying temperature of the 3D matrix. Attributed to these nice prop-

* Corresponding authors.
E-mail addresses: chenzhijun@nefu.edu.cn (Z. Chen), lishujun@nefu.edu.cn (S. Li).

https://doi.org/10.1016/j.cclet.2021.08.075
1001-8417/

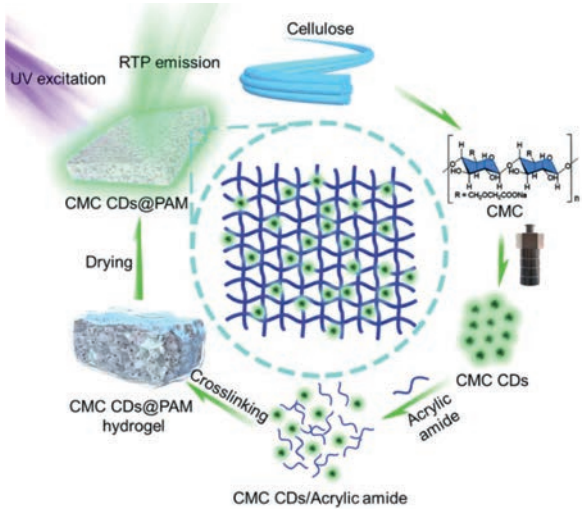

Scheme 1. Schematic representation showing design principle for CMC CDs@PAM composites.

erties, CMC CDs@PAM was successfully used to prepare RTP fibres for flexible luminescent textiles, which had great potential in future displaying devices and sensors.

CMC CDs were synthesized as previously described [32] and characterized by TEM, XPS, XRD and FT-IR (Figs. S1-S4 in Supporting information). TEM images showed that the CMC CDs had a diameter of 2-5 nm (Fig. S1) and the XPS and FT-IR spectrum showed that their surface was decorated with C-C, C=C, C-O, C=O and C-N moieties, in agreement with our previous reports (Figs. S2-S4). The UV-vis absorption spectrum of CMC CDs dispersed in water showed two major absorption bands, located at 280 nm and 360 nm. These originate from $\pi \rightarrow \pi^*$ and $n \rightarrow \pi^*$ transitions and are associated with C=C bonds and lone pairs on N atoms, respectively (Fig. 1a, red line). Under irradiation with 365 nm UV light, the aqueous dispersion of CMC CDs emitted bright green fluorescence, with an emission peak centered at 490 nm (Fig. 1a, black line) and a fluorescence lifetime of 11.09 ns (Fig. 1b). To enhance phosphorescence emission at room temperature, the phosphors should be efficiently restricted in rigid matrices. Herein, CMC CDs were polymerized *in situ* with MBA (crosslinker) and AM (monomer), using radical chemistry. TEM images showed that the CMC CDs were well dispersed in a 3D PAM network (Figs. 1c and d). SEM images of CMC CDs@PAM showed that incorporation of CMC CDs tightened the 3D network structure of the PAM (Fig. S5 in Supporting information). Significant RTP could be observed with the naked eye when CMC CDs@PAM was irradiated with 365 nm UV light (Fig. 1e). The overlap of the afterglow excitation spectrum and the absorption spectrum over the range of 350-400 nm shows that the phosphorescence originates mainly from C=O bonds in the CMC CDs (Fig. S6 in Supporting information) [32]. This is because carbonyl groups enhance the spin-orbital coupling (SOC) needed for phosphorescence emission. More interestingly, in addition to excitation-dependent fluorescence, CMC CDs@PAM also showed excitation-dependent phosphorescence. The afterglow emission of CMC CDs@PAM peaked largely at 535 nm and gradually red-shifted to 545 nm as the excitation wavelength was increased (Fig. 1f). Because of this phenomenon, we recorded the delayed emission spectra and phosphorescence lifetimes of CMC CDs@PAM at different temperatures. As the temperature was increased from 100 K to 300 K, the intensity of the afterglow emission of CMC CDs@PAM declined (Fig. S7a in Supporting information), because phosphorescence was reduced by increased non-radiative deactivation at elevated temperatures. The phosphorescence lifetime showed a corresponding decrease, from 2.6 s to 674.91 ms, as the temperature was increased (Figs. S7b-f in Supporting information).

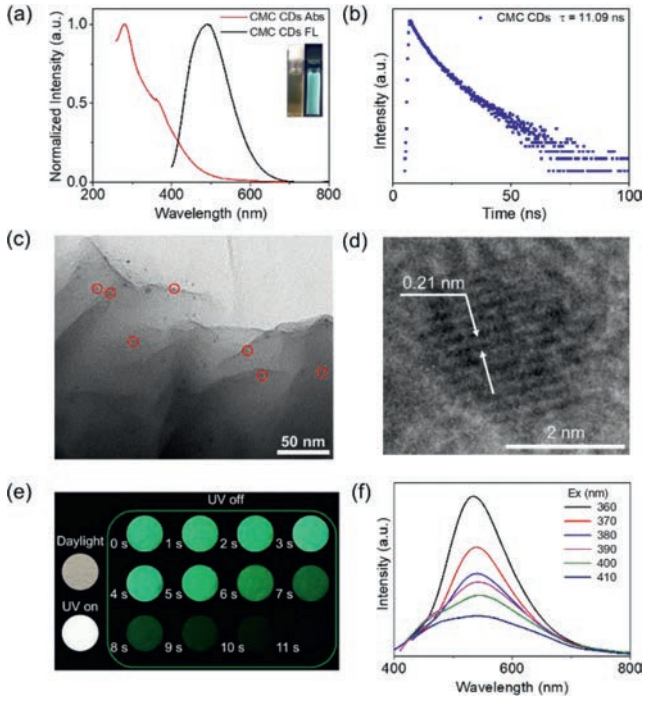

Fig. 1. (a) Normalized UV-vis absorbance (red line) and fluorescence emission (black line, λ_{ex} = 380 nm) spectra of CMC CDs solution (insets show CMC CDs solution under daylight and 365 nm UV light. (b) Fluorescence lifetime (τ) of CMC CDs solution monitored at 490 nm (λ_{ex} = 380 nm). (c) TEM image of CMC CDs@PAM with some individual carbon dots indicated by red circles (scale bar = 50 nm). (d) high resolution TEM image of single CMC CD in CMC CDs@PAM (scale bar = 2 nm). (e) Corresponding photographs of CMC CDs@PAM under daylight, 365 nm UV lamp on and off. (f) Phosphorescence of CMC CDs@PAM upon excitation with wavelengths from 360 nm to 410 nm.

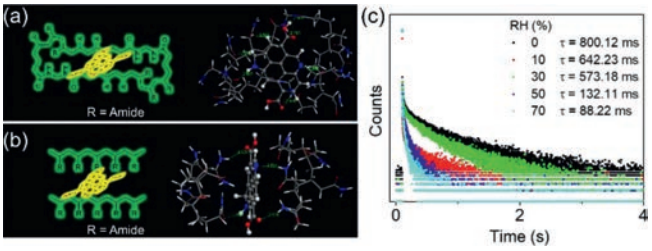

Fig. 2. Mechanism of RTP emission. (a) Molecular interaction between the model of CMC CDs and 3D PAM molecular network. (b) Molecular interaction between the model of CMC CDs and polyacrylamide chains. (c) Lifetime decay profiles of RTP of CMC CDs@PAM polymer composite under conditions of different relative humidity (λ_{ex} = 370 nm).

Several control experiments were conducted to determine the mechanism of RTP emission by CMC CDs@PAM. No RTP was observed upon UV irradiation when CMC CDs were physically mixed with polyacrylamide (Fig. S8 in Supporting information). SEM images also showed that there was a flat film morphology and no dense 3D structure between physically mixed CDs and acrylamide (Fig. S9 in Supporting information), showing that 3D molecular confinement of CMC CDs is necessary for RTP emission. DFT calculation was also used to investigate this phenomenon. The model of 3D molecular network (3D PAM) formed more hydrogen bonds with molecular model of CMC CDs (7 per interaction), compared to the interaction between molecular model of CMC CDs and polymer chain (polyacrylamide) (4 per interaction) (Figs. 2a and b). As a result, 3D molecular network had stronger binding energy with CMC

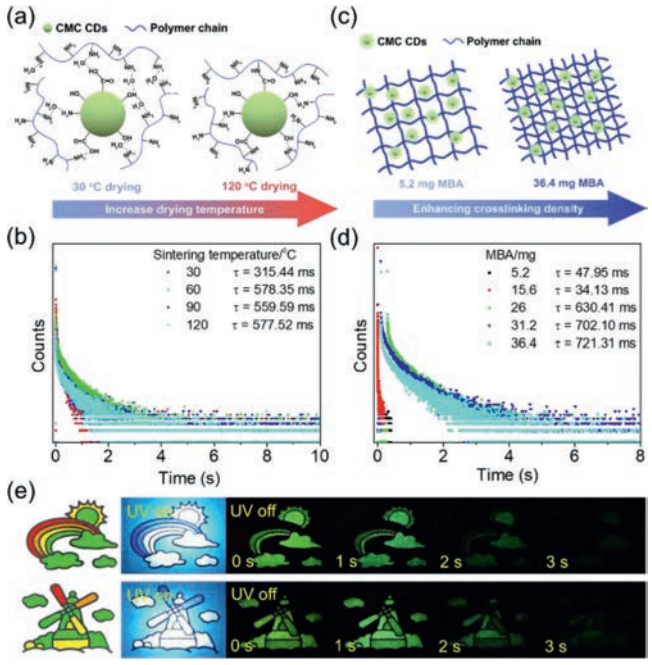

Fig. 3. Tuning RTP lifetime. (a) Schematic representation of CMC CDs@PAM following drying at different temperatures. (b) Luminescence decay curves monitored at 540 nm (λ_{ex} = 370 nm) of CMC CDs@PAM dried at 30 °C, 60 °C, 90 °C and 120 °C. (c) Schematic representation of CMC CDs@PAM with different crosslinking densities. (d) Lifetime decay profiles of CMC CDs@PAM with increasing crosslinking densities (λ_{ex} = 370 nm). (e) Digital photographs of encrypted images created using PAM (red), physical blend of CMC CDs and PAM (orange), CMC CDs@PAM dried at 30 °C (yellow) and CMC CDs@PAM dried at 60 °C (green). Photographs were taken under irradiation with 365nm UV lamps and at different times after switching off the lamps.

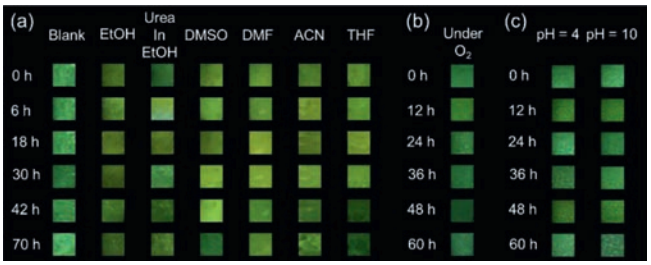

Fig. 4. Photostability of RTP emission. (a) Photographs of afterglow emission of CMC CDs@PAM in different solvents (EtOH, urea in EtOH, DMSO, DMF, ACN and THF) after removing UV light source (λ_{ex} = 360 nm). (b) Photographs of afterglow emission of CMC CDs@PAM in oxygen environment after removing UV light source (λ_{ex} = 360 nm). (c) Photographs of afterglow emission of CMC CDs@PAM in acidic (pH 4) and alkaline (pH 10) solution after removing UV light source (λ_{ex} = 365 nm). All experiments were carried out at room temperature.

CDs (–2.01 eV), compared to the binding energy between CMC CDs and polymer chains (–1.74 eV). These results strongly suggest that CMC CDs only produce RTP when firmly anchored in a suitable polymer matrix by strong hydrogen bonds. To further investigate this hypothesis, CMC CDs@PAM was exposed to humidity, which could weaken and even break down hydrogen bonding interactions. Exposure of powdered CMC CDs@PAM to increasing relative humidity (RH) reduced the lifetime of emission (800.12 ms, 642.23 ms, 573.18 ms, 132.11 ms and 88.21 ms at RH = 0%, 10%, 30%, 50% and 70%, respectively, Fig. 2c). As expected, humidity weakened the hydrogen bonds between the CMC CDs and PAM matrix, leading to reduced RTP emission. All of these results demonstrate that 3D molecular confinement and strong hydrogen bonding are crucial for RTP emission.

The RTP lifetime of CMC CDs@PAM could be finely tuned by either drying or varying the amount of crosslinking agent in the composite polymer. The RTP lifetime was increased by drying at higher temperatures. Specifically, the RTP lifetime of CMC CDs@PAM increased from 315.44 ms to 577.52 ms when the drying temperature was increased from 30 °C to 120 °C (Figs. 3a and b), probably because the higher temperature led to tighter confinement of the CMC CDs within the 3D PAM matrix [47]. Notably, when the drying temperature reached over 60 °C, the lifetime was increased slowly. This might because that the incorporated water molecules in the CMC CDs@PAM has been almost completely evaporated at 60 °C, which triggered a tight interaction between molecular network and CDs and produced efficient RTP emission. As a result, further heating did not efficiently increase the interaction force between the 3D matrix and CMC CDs, which only produced slow increase of lifetime. As a control, PAM has no obvious phosphorescence with the increase of temperature (Fig. S10 in Supporting information). The RTP lifetime was also increased by enhancing crosslinking within the PAM by increasing the proportion of MBA crosslinkers (Figs. 3c and d). Increasing the amount of crosslinking within the PAM matrix is also likely to lead to tighter confinement of the CMC CDs within the polymer matrix. Notably, increased concentration of MBA at low concentration range did not always enhance the lifetime. We proposed that the MBA might play as a substitute for CMC CDs at a low concentration range, to form hydrogen bonding with molecular matrix since MBA had abundant amide moieties. This result decreased the interaction force between CMC CDs and matrix, which finally decreased the RTP lifetime. As a visual demonstration of this tunable lifetime, CMC CDs@PAM was designed as a time-resolved image. PAM, a physical blend of CMC CDs and PAM, and CMC CDs@PAM dried at different temperatures were loaded onto different positions of the image (Fig. 3e). Upon excitation with a 365 nm UV lamp, a white-blue pattern of a landscape became clearly visible. Once the lamp was turned off, the image immediately changed and, because of variations in the afterglow lifetime of the different polymers, the image also evolved with time. When the lamp was turned off, the portions of the image filled with PAM (red in original image) and a physical blend of CMC CDs and PAM (orange in original image) immediately became invisible because of the short lifetimes of the RTP in the absence of hydrogen bonding. One second after turning off the lamp, the phosphorescence intensity of CMC CDs@PAM dried at 30 °C (yellow in original image) is clearly less that of CMC CDs@PAM dried at 60 °C (green in original image), indicating a shorter phosphorescence lifetime. Residual RTP lasted for several seconds and could be clearly seen with the naked eye.

Because they are protected by the 3D PAM network, the CMC CDs phosphors within CMC CDs @PAM have excellent antiquenching properties and exceptional stability. As-prepared CMC CDs@PAM powder was first dispersed in different polar organic solvents: ethyl alcohol (EtOH), a saturated ethanolic solution of urea (urea in EtOH), dimethyl sulfoxide (DMSO), *N,N*-dimethylformamide (DMF), acetonitrile (ACN) and tetrahydrofuran (THF) (Fig. 4a). Although it is surprising that the RTP is not quenched by these polar solvents, a very long lifetime afterglow could be observed with the naked eye (Fig. 4a and Fig. S11 in Supporting information). In order to further investigate the extraordinary stability of CMC CDs@PAM phosphors, solid composite, obtained by freeze drying, was next exposed to oxygen or dissolved in ethanol at different pH. The phosphors retained excellent stability in both an oxygen environment (Fig. 4b) and under different pH conditions (Fig. 4c). These results indicate that the fabricated CMC CDs@PAM phosphors have exceptional stability. Protection by the 3D PAM network prevents quenching of the CMC CDs, which

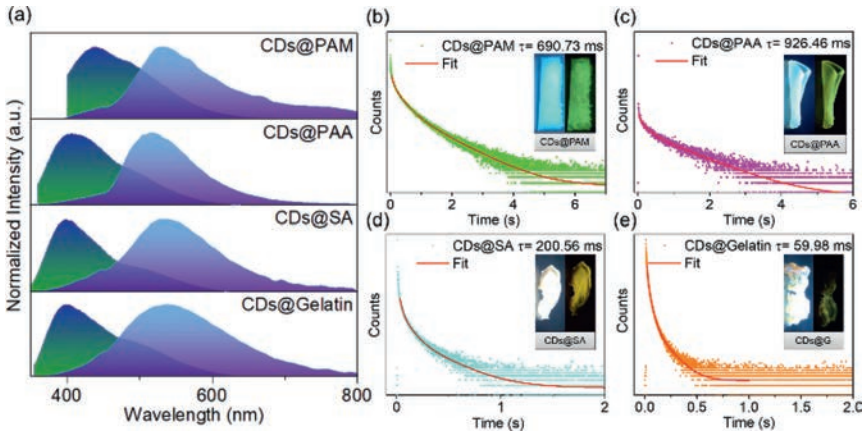

Fig. 5. Photophysical properties of CMC CDs@PAM, CMC CDs@PAA, CMC CDs@SA and CMC CDs@Gelatin under ambient conditions. (a) Normalized fluorescence (green) and phosphorescence spectra (purple). CMC CDs@PAM: delay time = 10 ms, λ_{ex} = 370 nm; CMC CDs@PAA: delay time = 8 ms, λ_{ex} = 365 nm; CMC CDs@SA: delay time = 5 ms, λ_{ex} = 330 nm; CMC CDs@Gelatin: delay time = 5 ms, λ_{ex} = 335 nm). (b-e) Phosphorescence decay of CMC CDs@3D polymer at room temperature (inset photographs show CMC CDs@3D polymer taken with the 365 nm UV lamp turned on (left) and off (right)).

means that the CMC CDs@PAM phosphors are suitable for various applications under different environmental conditions.

The experimental results reported above describe a facile and cost-effective method for fabricating efficient PAM-based RTP materials with tunable lifetimes. Importantly, this method can easily be expanded to other 3D molecular matrices. Acrylic acid (AA), sodium alginate (SA) and gelatin were used to prepare CMC CDs@3D polymers (CMC CDs@PAA, CMC CDs@SA and CMC CDs@Gelatin, respectively). SEM images show their porous 3D structures (Figs. S12-S14 in Supporting information). The phosphorescence spectra of the three new materials were all similar to that CMC CDs@PAM, with emission peaks at ~535 nm (Fig. 5a). As in the case of CMC CDs@PAM, the three new materials all emitted blue fluorescence when irradiated at 365 nm and yellow ultra-long phosphorescence that could be observed with the naked eye when the UV lamp was switched off (Figs. 5b-e). Interestingly, CDs@Gelatin showed the shortest lifetime during all the samples. This might be attributed to the absence of chemical crosslinker in the matrix, which could not produce a tight interaction between CDs and gelatin. These results demonstrated that as-developed 3D confinement strategy was general for wide ranging of matrix.

As a demonstration of the application, CMC CDs@PAM was used for preparing flexible RTP fibres, considering of the factor that RTP fibres played extremely important roles in the flexible displaying devices and sensors [48-51]. To achieve the goal, an automated apparatus was designed for preparing RTP fibres using CMC CDs@PAM, containing cotton fibres, dip-coating tank and collection roller (Fig. 6a). During the process, cotton fibres firstly passed through the coating tank filled with hydrogel precursor (Video S1 in Supporting information). After that, the precursor solution coated cotton fibres were *in situ* crosslinked and dried by heating plate (Video S1). In such manner, RTP fibres were obtained (Fig. 6a and Video S1). SEM images showed that as-obtained fibres were evenly coated with CMC CDs@PAM (Fig. S15 in Supporting information). As-obtained fibres showed nice RTP emission (Fig. 6b). Moreover, RTP fibres had nice stability and maintained the RTP emission after sinking them in the organic and aqueous solvent for 24 h (Fig. 6c). This result suggests these RTP fibres were stable and could be used practically. Encouraged by this, RTP fibres were used for embroidery assisted by commercial machine (Fig. S16 and Video S2 in Supporting information). As expected, as-obtained embroidery showed nice RTP emission (Fig. 6d). All these results demonstrated our design for preparing RTP materials were effective and could be large-scaly used in the practical applications.

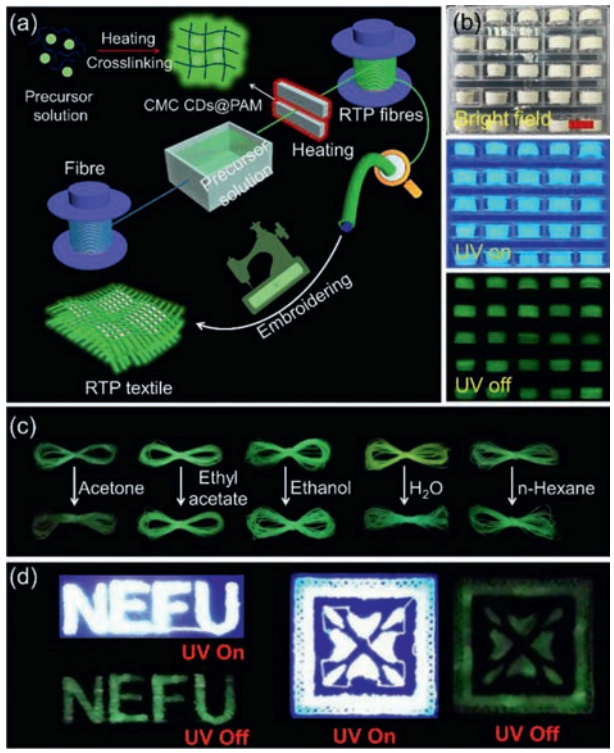

Fig. 6. Application of CMC CDs@PAM. (a) Schematic illustration of preparation of RTP fibres *via* home-made apparatus. (b) Digital images of RTP fibres under bright field, UV irradiation and after turning off the UV sources, scale bar = 1 cm. (c) RTP emission of fibre before and after treatment of the corresponding solvent for 24 h (The photo was taken after drying the treated fibres at 60 °C for 2 h.). (d) Digital images of embroidery upon and after UV excitation.

In summary, we have developed a facile and general 3D confinement strategy that can produce robust, tunable, long-lived RTP emission. Because the strength of the interaction between CMC CDs and PAM can be varied by simply altering the degree of crosslinking or the sintering temperature, we were able to prepare a series of CMC CDs@PAM composites with different RTP lifetimes, ranging from 34.13 ms to 926.46 ms. The external 3D network also enabled unquenched emission by CMC CDs@PAM in organic solvents and in an oxygen environment. We used the excellent, tunable RTP emission of CMC CDs@PAM to develop a method for preparing functional RTP fibres used for luminescent textiles. We

believe that this work not only provides a method for the preparation of easily-produced, readily tunable RTP materials but also provides a general route to CDs-based RTP materials.

Declaration of competing interest

The authors declare that they have no known competing financial interests or personal relationships that could have appeared to influence the work reported in this paper.

Acknowledgments

This work was supported by the National Natural Science Foundation of China (No. 31890774), Excellent Young Scholar Sponsorship Program by National Forestry and Grassland Administration of China Funding (No. 2019132611), Heilong Jiang Postdoctoral Science Foundation (No. LBH-Z18005), Young Elite Scientists Sponsorship Program by CAST (No. 2018QNRC001).

Supplementary materials

Supplementary material associated with this article can be found, in the online version, at doi:10.1016/j.cclet.2021.08.075.

References

[1] X. Yang, D. Yan, Chem. Sci. 7 (2016) 4519–4526.
[2] X. Ma, J. Wang, H. Tian, Acc. Chem. Res. 52 (2019) 738–748.
[3] L. Ma, S. Sun, B. Ding, Adv. Funct. Mater. 31 (2021) 2010659.
[4] G Wang, Z Wang, B Ding, Chin. Chem. Lett. 32 (2021) 3039–3042.
[5] K. Jiang, Y. Wang, C. Cai, Adv. Mater. 30 (2018) 1800783.
[6] K. Jiang, Y. Wang, X. Gao, Angew. Chem. Int. Ed. 57 (2018) 6216–6220.
[7] X. Li, G. Baryshnikov, C. Deng, Nat. Commun. 10 (2019) 731.
[8] Y. Su, S.Z.F. Phua, Y. Li, Sci. Adv. 4 (2018) eaas9732.
[9] J. Wang, X. Gu, H. Ma, Nat. Commun. 9 (2018) 2963.
[10] Z. An, C. Zheng, Y. Tao, Nat. Mater. 14 (2015) 685–690.
[11] T Feng, S Zhu, Q Zeng, ACS Appl. Mater. Interfaces 10 (2017) 12262–12277.
[12] B. Wang, Y. Mu, H. Zhang, ACS Cent. Sci. 5 (2019) 349–356.
[13] S. Tao, S. Lu, Y. Geng, Angew. Chem. Int. Ed. 57 (2018) 2393–2398.
[14] X. Zhou, H. Liang, P. Jiang, Adv. Sci. 3 (2016) 1500155.
[15] P. Long, Y. Feng, C. Cao, Adv. Funct. Mater. 28 (2018) 1800791.
[16] L. Gu, H. Wu, H. Ma, Nat. Commun. 11 (2020) 944.
[17] N. Gan, H. Shi, Z. An, Adv. Funct. Mater. 28 (2018) 1802657.
[18] X. Dong, L. Wei, Y. Su, J. Mater. Chem. C 3 (2015) 2798–2801.
[19] Z. Wang, T. Li, B. Ding, X. Ma, Chin. Chem. Lett. 31 (2020) 2929–2932.
[20] M.S. Kwon, Y. Yu, C. Coburn, A.W. Phillips, Nat. Commun. 6 (2015) 8947.
[21] B. Wu, N. Guo, X. Xu, Adv. Opt. Mater. 8 (2020) 2001192.
[22] H. Wu, W. Chi, Z. Chen, Adv. Funct. Mater. 29 (2019) 1807243.
[23] G. Zhang, G.M. Palmer, M. Dewhirst, Nat. Mater. 8 (2009) 747–751.
[24] S. Lu, L. Sui, J. Liu, Adv. Mater. 29 (2017) 1603443.
[25] B. Wang, J. Li, Z. Tang, Sci. Bull. 64 (2019) 1285–1292.
[26] W. Li, Y. Liu, B. Wang, Chin. Chem. Lett. 30 (2019) 2323–2327.
[27] B. Wang, J. Yu, L. Sui, Adv. Sci. 8 (2021) 2001453.
[28] J. Liu, N. Wang, Y. Yu, Sci. Adv. 3 (2017) e1603171.
[29] Q. Li, M. Zhou, Q. Yang, Chem. Mater. 28 (2016) 8221–8227.
[30] Y. You, K. Huang, X. Liu, Small 16 (2020) 1906733.
[31] K. Jiang, Y. Wang, C. Cai, Chem. Mater. 29 (2017) 4866–4873.
[32] P. Wang, D. Zheng, S. Liu, Carbon 171 (2021) 946–952.
[33] Y. Deng, D. Zhao, X. Chen, Chem. Commun. 49 (2013) 5751–5753.
[34] K. Jiang, L. Zhang, J. Lu, Angew. Chem. Int. Ed. 128 (2016) 7347–7351.
[35] Z. Tian, D. Li, E.V. Ushakova, Adv. Sci. 5 (2018) 1800795.
[36] Y. Chen, J. He, C. Hu, J. Mater. Chem. C 5 (2017) 6243–6250.
[37] J. Tan, J. Zhang, W. Li, J. Mater. Chem. C 4 (2016) 10146–10153.
[38] K. Patir, S.K. Gogoi, ACS Sustain. Chem. Eng. 6 (2018) 1732–1743.
[39] X. Kong, X. Wang, H. Cheng, J. Mater. Chem. C 7 (2019) 230–236.
[40] J. Joseph, A.A. Anappara, Phys. Chem. Chem. Phys. 19 (2017) 15137–15144.
[41] J. Tan, R. Zou, J. Zhang, Nanoscale 8 (2016) 4742–4747.
[42] H. Gou, Y. Liu, G. Zhang, Nanoscale 11 (2019) 18311–18319.
[43] K. Jiang, Y. Wang, Z. Li, Mater. Chem. Front. 4 (2020) 386–399.
[44] Y. Yu, Z. Mu, B. Jin, Angew. Chem. Int. Ed. 59 (2020) 2071–2075.
[45] M. Jiang, X. Liu, Z. Chen, iScience 23 (2020) 100832.
[46] Y. Gao, K. Wu, Z. Suo, Adv. Mater. 31 (2019) 1806948.
[47] X. Bao, E.V. Ushakova, E. Liu, Nanoscale 11 (2019) 14250–14255.
[48] X. Shi, Y. Zuo, P. Zhai, Nature 591 (2021) 240–245.
[49] X. Zhang, L. Du, W. Zhao, Nat. Commun. 10 (2019) 5161.
[50] J. Li, B. Wang, H. Zhang, Small 15 (2019) 1805504.
[51] Y. Li, M. Gecevicius, J. Qiu, Chem. Soc. Rev. 45 (2016) 2090–2136.